engineering proceedings

MDPI

Proceeding Paper

Statistical Analysis of Gyroscopic Data to Determine Machine Health in Additive Manufacturing †

Alexander Isiani [1], Lelend Weiss [2] and Kelly Crittenden [3,*]

[1] Affiliation 1; aci004@latech.edu
[2] Affiliation 2; lweiss@latech.edu
[2] Affiliation 3
* Correspondence: kellyc@latech.edu.edu
† Presented at the 10th International Electronic Conference on Sensors and Applications (ECSA-10), 15–30 November 2023; Available online: https://ecsa-10.sciforum.net/.

Abstract: Additive manufacturing, commonly known as 3D printing, has significantly advanced component production across multiple industry sectors. Despite its numerous benefits, including reduced lead times and the ability to produce complex geometries, a few obstacles still prevent widespread adoption. Current research efforts have predominantly focused on *in-situ* monitoring and investigating the mechanical properties of 3D printed materials, with limited attention given to the sources of skewness in the fabricated products. To address this gap, our study aims to explore the factors contributing to skewness in 3D-printed objects. Specifically, we examine the influence of the belt and carriage wheel conditions within the 3D printer on the shape of the fabricated products, resulting from potential distortions in the orientation of the print head carriage during the printing process. A comprehensive analysis was employed, utilizing One-Way ANOVA, Tukey, Fisher Least Significant Difference Method, and Friedman Rank test, to establish statistically significant evidence supporting the notion that the mechanical components, namely the belt, and wheel, have a substantial impact on the orientation of the print head, consequently leading to skewness in the final 3D printed products.

Keywords: print head carriage; gyroscope; skewness; additive manufacturing

Citation: Isiani, A.; Weiss, L.; Crittenden, K. Statistical Analysis of Gyroscopic Data to Determine Machine Health in Additive Manufacturing. *Eng. Proc.* **2023**, *56*, x. https://doi.org/10.3390/xxxxx

Academic Editor(s):

Published: 15 November 2023

1. Introduction

3D Printing, also known as Additive Manufacturing (AM), is an innovative and transformative technology that has the potential to disrupt traditional design and manufacturing practices developed over the past two centuries [1,2]. AM has been implemented in the fields of optics [3], construction [4], medicine [5,6], food processing [7], Dental [8,9], Biotechnology [10], Mechanical systems [11–14], Aerospace [15], Automobile [16–18], Electrical [19,20], Electronic [21–23], and Fashion[24,25]. Although 3D printing offers various advantages, such as decreased lead times and the ability to produce intricate geometries, several barriers remain to hinder its widespread adoption. Extensive research efforts have been undertaken to characterize the mechanical properties [26–31] and thermal properties [32–36] and establish reliable quantification methods for 3D printed components [37–41].

Researchers have conducted extensive investigations into using various sensors, including accelerometers [42–44], cameras [45,46], acoustic emission sensors[47,48], and thermocouples [49–52], for in situ monitoring. Through these studies, it has been consistently observed that employing *in situ* monitoring techniques enables the prediction of the health condition of 3D printers and facilitates the detection of defects in the quality of the printed products. Sensing systems are crucial for the effectiveness of *in situ* monitoring

systems; however, their capability to accurately attribute a signal to a specific fault source is constrained by their signals' limited "uniqueness" [53]. Researchers have investigated the mechanical properties of 3D printed components, specifically examining factors such as tensile strength [54], nozzle temperature [55], infill orientation [56], printing speed, and feed rate [57]. The findings of this study revealed that the upright infill orientation demonstrated the lowest mechanical properties, whereas the on-edge and flat infill orientations exhibited the highest levels of mechanical strength [12].

The literature reviewed above encompasses recent endeavors to investigate *in situ* monitoring techniques and mechanical properties of structures produced through Fused Filament Fabrication (FFF) 3D printing technologies. While substantial efforts have been devoted to evaluating material properties, a noticeable gap exists in understanding the influence of print head orientation during fabrication. Furthermore, research regarding the effects of different belt and wheel parameters on the performance of 3D printers has been scarce up to this point.

This study undertakes an experimental endeavor to assess the print head orientation and carriage condition of a 3D printer. Additionally, it investigates the impact of belt and wheel parameters. The findings of this research offer valuable insights into understanding the influence of these factors on the overall performance of the 3D printing process.

This article is structured as follows: Section 2 presents an overview of the experimental setup utilized in this study. Section 3 provides a detailed explanation of the experimental design techniques employed. The findings and discussions derived from the experiments are presented in Section 4. Finally, Section 5 concludes the article with a summary of the key outcomes and provides concluding remarks based on the current work.

2. Experimental Setup

Figure 1 illustrates the experimental setup employed for the statistical analysis. A Bowden tube style Fused Filament Fabrication (3D printing) machine manufactured by Creality (the Ender 3) was utilized to observe the movement of the print head carriage. A 3-axis MPU6050 Accelerometer/Gyroscope sensor was mounted on the carriage of the printer to capture the angular velocity and acceleration data as the print head traversed the y-axis of the machine. The sensor was connected to an Arduino Uno microcontroller for data acquisition. To ensure data integrity, an SD shield and a Laptop were employed to record and save the collected data. The recorded data comprised different angular velocities corresponding to belt and carriage wheel conditions. Statistical analysis was conducted to evaluate the significance of these recorded angular velocities.

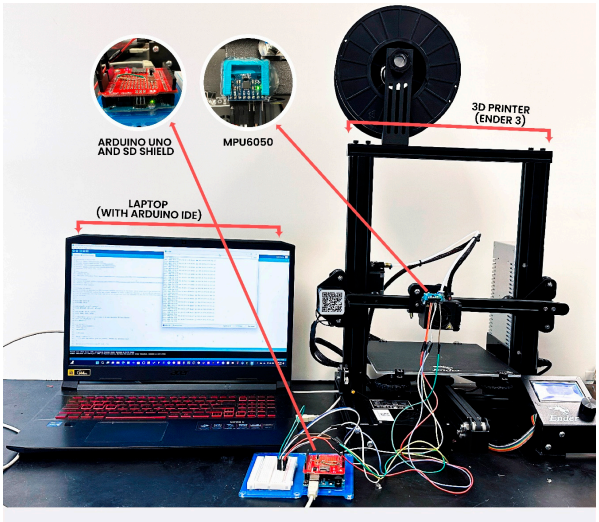

Figure 1. Experimental setup used for checking for the factors contributing to skewness in 3D printed samples.

3. Experimental Design

The experimental setup depicted in Figure 1 was utilized with minor modifications applied to the belt and carriage wheel configurations, as shown in Figure 2. These variations allowed for examining the print head carriage under different conditions, aiding in a comprehensive assessment of its performance. These conditions are stated thus:

a. **Leveled Belt–Tight Wheel**: This is the state desired for the 3-D printer to maintain as it fabricates products. This condition ensures stable orientation of the printer carriage head as it moves from one point to the other in the x, y, and z directions. In addition, the eccentric nut holding the wheel, which drives the carriage is well-tightened while the belt is leveled.
b. **Unleveled Belt–Tight Wheel**: This condition is achieved by creating bumps along the belt path to observe what happens when the carriage is slightly misoriented.
c. **Leveled Belt–Loose Wheel**: This condition makes the carriage head tilt and generates an inconsistent orientation as it moves along the reel because of loosed wheels, although the belt is leveled.
d. **Unleveled Belt–Loose Wheel**: This is an extreme case where the belt and wheels are unstable

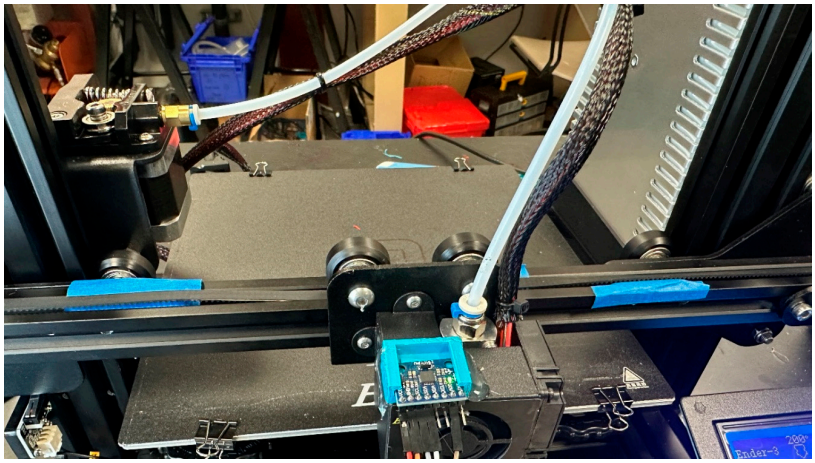

(**a**)

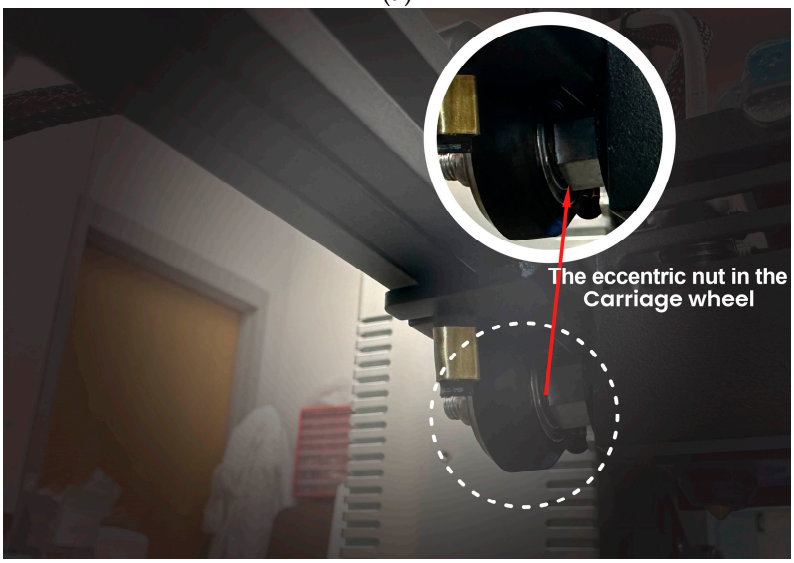

(**b**)

Figure 2. (**a**). The print head carriage, along with the integration of an MPU6050 sensor and blue tapes placed to interrupt the belt path. (**b**). The eccentric nut in the carriage wheel, which was intentionally varied during the course of the experiment.

This study analyzed the conditions based solely on the recorded angular velocity data obtained from the MPU6050 sensor. The focus was primarily on the changes in the orientation of the print head carriage. By utilizing the angular velocity data, much insight would be gained through the rotational motion of the carriage during different experimental conditions. This approach allowed the examination of how variations in orientation affected the performance and behavior of the print head carriage. The analysis of the recorded angular velocity data served as a valuable tool in understanding the dynamics and characteristics of the print head carriage in relation to its orientation changes.

The data collection process commenced immediately after the default calibration routine, which involved a 15-nd pause on the print head carriage to calibrate its orientation. Subsequently, the carriage was driven back and forth along the x-axis of the reel, covering a distance of 100 mm. The speed of this movement was set at 1000 mm/min for a duration of one minute and thirty seconds. Throughout this motion, a total of 1500 data points were recorded and saved in the laptop's storage for subsequent analysis. The recorded data points captured the relevant variables (x, y, and z angular velocity) necessary for evaluating the performance and behavior of the print head carriage during the specified movement scenario. These data points will be subjected to thorough analysis and examination to extract meaningful insights and draw valid conclusions regarding the carriage's orientation and motion characteristics. The equations employed for checking statistical evidence and determining significance will be elaborated in Appendix A.

3. Result and Discussion

The analysis in this study involved reducing the initial dataset of 1500 data points into 30 data points. This reduction was achieved by segmenting the collected data into sections of 50 data points each. This reduction aimed to streamline the dataset for further analysis and interpretation. Firstly, the correlation matrix in Figure 3 presented a comprehensive overview of the correlations between root mean square (RMS) values of the different explore conditions, allowing for determining the degree of correlation. By examining the correlation coefficients, we can evaluate whether the variables exhibit perfect, strong, or weak correlations with each other.

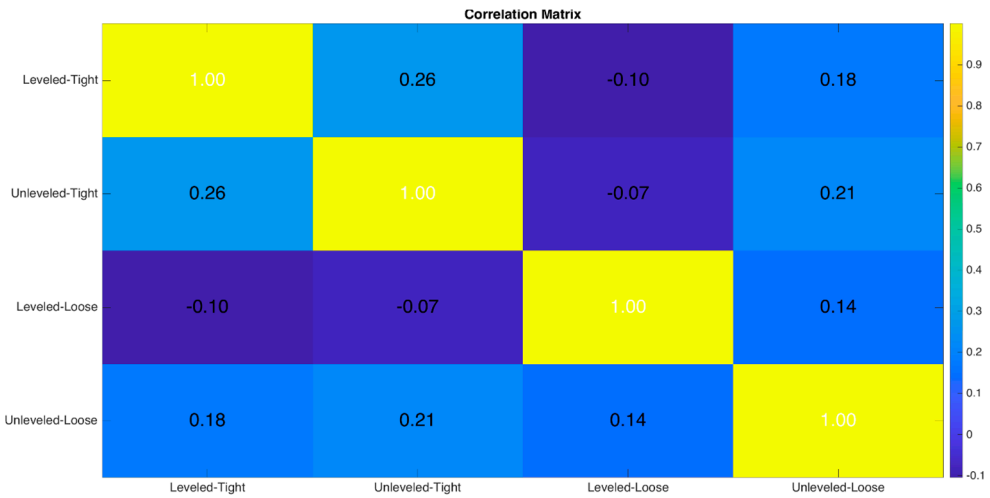

Figure 3. The correlation matrix for Leveled Belt-Tight Wheel condition, Unleveled Belt-Tight Wheel condition, Leveled Belt-Loose Wheel condition, and Unleveled Belt-Loose Wheel condition.

The correlation matrix analysis revealed that either uncorrelated or weak correlations were observed among the data collected for each condition. This finding suggests that variations in the condition of the belt and wheel of the 3D printer directly corresponded to changes in the orientation of the print head carriage. The lack of strong correlations or the presence of weak correlations between the collected data indicates that

alterations in the belt and wheel conditions had a noticeable influence on the orientation of the print head carriage. As the condition of the belt and wheel changed, the orientation of the carriage exhibited corresponding adjustments. These results highlight the direct relationship between the belt and wheel conditions and the orientation of the print head carriage.

Figure 4 presents the normality test graphs generated using Minitab software. These graphs are based on the reduced data points corresponding to the four different conditions examined in the study. The normality test determines the distributional characteristics of the data, thereby facilitating the selection of appropriate parametric or non-parametric statistical tests for further analysis. Table 1 provides the descriptive statistics for each of the conditions investigated. The combination of the normality test graphs from Figure 3 and the descriptive statistics presented in Table 1 assists in elucidating the nature of the collected data and determining the appropriate statistical methods for subsequent analyses.

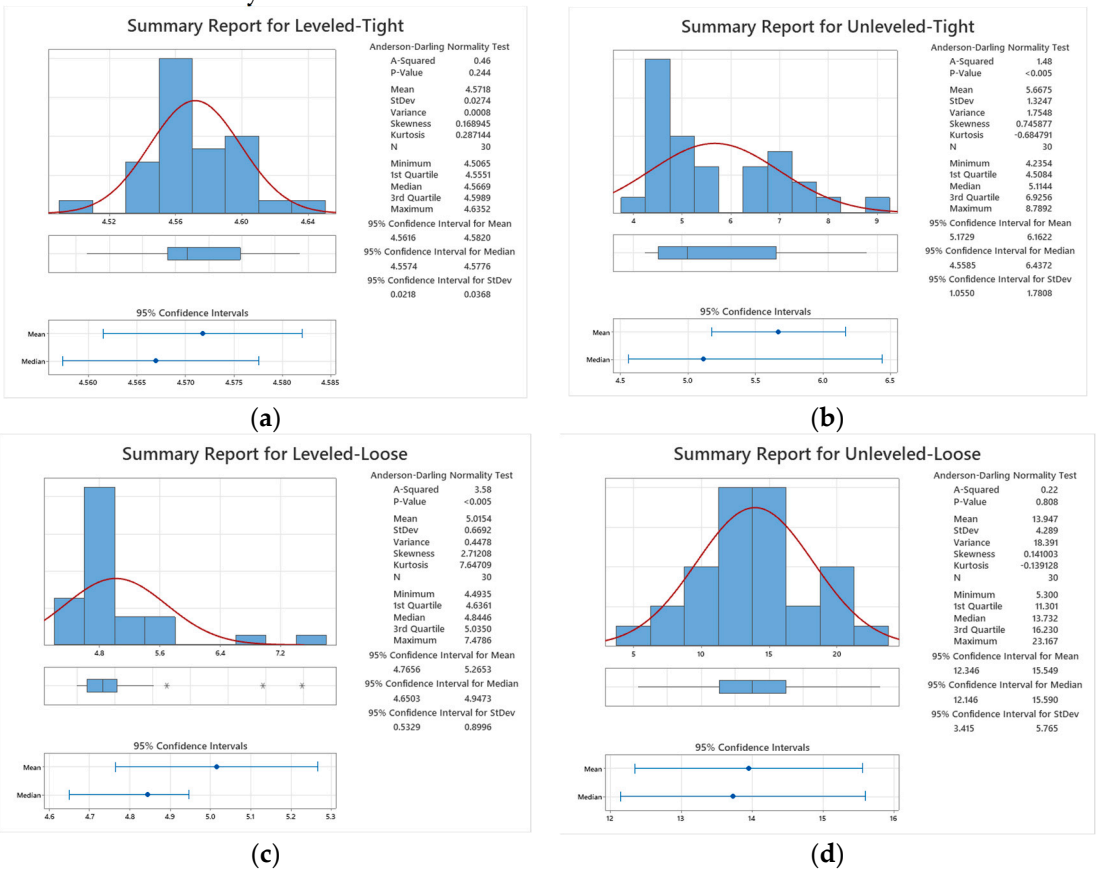

Figure 4. The descriptive statistics summary report and normality plot for (**a**) Leveled Belt-Tight Wheel condition; (**b**) Unleveled Belt-Tight Wheel condition; (**c**) Leveled Belt-Loose Wheel condition; (**d**) Unleveled Belt-Loose Wheel condition.

Table 1. shows the descriptive statistics with the p-value of the condition.

Conditions	Mean	Std. Dev.	Variance	*p*-Value
Leveled Belt–Tight Wheel	4.572	0.027	0.00075	0.244
Unleveled Belt–Tight Wheel	5.668	1.325	1.755	<0.005
Leveled Belt–Loose Wheel	5.015	0.669	0.448	<0.005
Unleveled Belt–Loose Wheel	13.947	4.289	18.391	0.808

The normality plots generated from the analysis indicate that the data for the conditions "Leveled Belt–Tight Wheel" and "Unleveled Belt–Loose Wheel" exhibit a normal distribution. The p-values associated with these conditions are 0.244 and 0.808, respectively. Conversely, the distribution of data for the other two conditions remains unknown. Based on these findings, the subsequent analysis can be conducted using parametric and non-parametric tests while considering a type 1 error, α, of 0.05. Since the data for the "Leveled Belt–Tight Wheel" and "Unleveled Belt–Loose Wheel" conditions follow a normal distribution, parametric tests such as One-Way Analysis of Variance (ANOVA), Tukey Pairwise Comparison, and Fisher-Least Significant Difference (LSD) methods were applied.

Table 2 illustrates the hypothesis and the significance level used for the parametric analysis. The one-way ANOVA result presented in Table 3 demonstrates the influence of the belt and wheel condition on the orientation of the print head, consequently affecting the shape of fabricated products. The obtained p-value of zero suggests rejecting the null hypothesis, indicating significant evidence supporting the assertion that a meaningful difference exists in the print head's mean root mean square (RMS) orientation based on the varying belt and carriage wheel conditions. These findings highlight the impact of the experimental conditions on the overall performance and behavior of the print head. By rejecting the null hypothesis, it can be inferred that the belt and carriage wheel condition plays a significant role in determining the orientation of the print head during the fabrication process. This observation underscores the importance of carefully selecting and optimizing the belt and wheel configurations to ensure consistent and accurate fabrication results.

Table 2. The hypothesis and type 1 error significance level.

Null hypothesis	All means are equal
Alternative hypothesis	Not all means are equal
Significance level	$\alpha = 0.05$

Table 3. Results from One-Way Analysis of Variance for the parametric machine conditions ("Leveled Belt–Tight Wheel" and "Unleveled Belt–Loosed Wheel").

Source	DF	Adj SS	Adj MS	F-Value	*p*-Value
Machine-Condition	1	1318.5	1318.46	143.37	0.000
Error	58	533.4	9.20		
Total	59	1851.8			

Table 5 presents the comparison results obtained using Tukey Pairwise Comparison and Fisher-Least Significant Difference (LSD) methods. These methods were employed to analyze and compare the grouping information of the two parametric conditions under investigation. The primary objective of employing these statistical methods was identifying significant differences between the various groups formed by the parametric conditions. Tukey Pairwise Comparison and Fisher-LSD methods are widely recognized and utilized in statistical analysis for conducting multiple pairwise comparisons between means.

Table 5a. Grouping Information Using the Tukey Method and 95% Confidence Interval (CI).

Machine-Condition	N	Mean	Grouping
Unleveled-Loose	30	13.947	A
Leveled-Tight	30	4.57180	B

Table 5b. Tukey Simultaneous Tests for Differences of Means.

Difference of Levels	Difference of Means	SE of Difference	95% CI	T-Value	Adjusted *p*-Value
Unleveled Belt-Loosed Wheel and Leveled Belt-Tight Wheel	9.375	0.783	(7.808, 10.943)	11.97	0.000

Table 5c. Grouping Information Using the LSD Method and 95% Confidence Interval (CI).

Machine-Condition	N	Mean	Grouping
Unleveled-Loose	30	13.947	A
Leveled-Tight	30	4.57180	B

Table 5d. Fisher Individual Tests for Differences of Means.

Difference of Levels	Difference of Means	SE of Difference	95% CI	T-Value	Adjusted *p*-Value
Unleveled Belt-Loosed Wheel and Leveled Belt-Tight Wheel	9.375	0.783	(7.808, 10.943)	11.97	0.000

Using Tukey's and LSD methods, similar results were obtained, indicating that the grouping information derived from the two machine conditions ("Leveled Belt–Tight Wheel" and "Unleveled Belt–Loose Wheel") is significantly distinct. These findings strongly imply that the state of the belt and gear components indeed influences the orientation of the print head carriage. The observed distinctions in grouping information suggest that there is evidence that variations in the state of the belt and gear have a notable impact on the orientation of the print head carriage.

However, a non-parametric analysis was conducted on the entire set of conditions using the Friedman Rank Test due to the unknown distribution of the "Unleveled Belt–Tight Wheel" and "Leveled Belt–Loose Wheel" conditions. This test is equivalent to a repeated measures ANOVA and is suitable for analyzing data when parametric assumptions are unmet. Tables 6 and 7 provide the descriptive statistics and test results obtained from the Friedman Rank Test. These tables offer valuable insights into the data and the outcomes of the statistical analysis. The results of the Friedman Rank Test revealed a significant rejection of the null hypothesis, as indicated by a *p*-value of zero. This finding indicates the presence of statistically significant evidence to support the assertion that the mean difference in the orientation of the carriages is indeed influenced by the gear and wheel conditions under investigation. These results further emphasize the importance of considering the gear and wheel components' condition when examining the carriages' orientation. By rejecting the null hypothesis, the analysis affirms that the gear and wheel conditions play a significant role in affecting the orientation of the carriages during the experimental procedures.

Table 6. The Descriptive Statistics from Friedman Rank Test.

Machine-Condition	N	Median	Sum of Ranks
Leveled-Loose	30	4.9493	70.0
Leveled-Tight	30	4.5211	41.0
Unleveled-Loose	30	13.3443	119.0

Unleveled-Tight	30	5.2660	70.0
Overall	120	7.0202	

Table 7. Hypothesis Test and Results from Friedman Rank Test.

Null hypothesis	H_0: All treatment effects are zero	
Alternative hypothesis	H_1: Not all treatment effects are zero	
DF	**Chi-Square**	***p*-Value**
3	62.84	0.000

Thus, based on the analysis conducted, it becomes evident that optimizing and fine-tuning the belt and wheel conditions is of utmost importance. This optimization is essential to achieve precise and accurate print head orientations, which, in turn, minimizes skewness in the 3D fabricated products. By focusing on enhancing the precision and accuracy of the print head orientation, the overall quality and reliability of the 3D printing process can be significantly improved. The findings from this study highlight the direct impact of the belt and wheel conditions on the orientation of the print head carriage. By carefully adjusting and optimizing these mechanical components, it becomes possible to minimize deviations and inaccuracies in the print head's movements. This, in turn, translates into improved outcomes in the final fabricated products, reducing any skewness that may occur during the printing process. Ultimately, by achieving precise print head orientations, manufacturers can ensure the production of high-quality and accurate 3D printed objects, meeting the desired specifications and minimizing any imperfections or inconsistencies.

4. Conclusions

Researchers have predominantly concentrated on studying the mechanical characteristics of 3D printed objects and monitoring them in real-time. This is due to the increasing prevalence of additively manufactured structures in dynamic applications. Consequently, it is crucial to identify the factors that contribute to irregularities in 3D printed products.

The primary objective of this study was to explore and understand the factors that contribute to skewness in 3D printed structures. In order to achieve this, the MPU6050 gyroscope was employed as a means to quantify the extent of variation in the root mean square orientation of the print head carriage during the fabrication process. Through rigorous analysis and experimentation, the findings of this study indicate that the condition of the belt and the wheel play a pivotal role in influencing skewness. This conclusion was derived from both parametric and non-parametric statistical analyses, which further underscore the significance of these factors. Overall, these results shed light on the key contributors to skewness in 3D printed products, providing valuable insights for improving such components' dynamic reliability and structural integrity. Further research and development in this area can help in innovative strategies and targeted interventions to mitigate skewness effectively, thereby resulting in a marked enhancement of the real-time quality of additively manufactured structures. By harnessing deeper insights into the underlying mechanisms, researchers and practitioners can collaboratively contribute to the establishment of a more refined and reliable additive manufacturing process. This, in turn, will pave the way for the creation of intricate, flawless, and precisely engineered components across various applications. Furthermore, future studies will delve extensively into the influence of the rheological and mechanical properties of the material during the fabrication process. This investigation is paramount as the printability of the material hinges significantly on the interplay between these two essential properties.

Author Contributions: Conceptualization, K.C. and A.I.; methodology, K.C. and A.I.; software, A.I.; validation, A.I., K.C., and L.W.; formal analysis, A.I.; investigation, A.I.; resources, K.C. and A.I.;

data curation, A.I.; writing—original draft preparation, A.I.; writing—review and editing, K.C., and L.W.; visualization, A.I.; supervision, K.C.; project administration, K.C. All authors have read and agreed to the published version of the manuscript.

Funding: This research received no external funding

Institutional Review Board Statement: The study did not require ethical approval.

Informed Consent Statement: The study did not involve the study of humans.

Data Availability Statement: The data are available in a publicly accessible repository. The data presented in the study are openly available at (will specify a location once publication is approved)

Conflicts of Interest: The authors declare no conflict of interest.

Appendix A

Mean, $\bar{x} = \frac{\sum_{i=1}^{n} x_i}{n}$

Variance, $s^2 = \frac{\sum_{i=1}^{n} (x_i - \bar{x})^2}{n-1}$

Standard Deviation, $s = \sqrt{\frac{\sum_{i=1}^{n} (x_i - \bar{x})^2}{n-1}}$

Parametric Test:

One-Way ANOVA assumes:

1. Completely randomized design and observations are mutually independent
2. Model errors are normally and independently distributed random variables
3. Variance constant for all levels of the factor

Sum of Squares (SS)

$$SS_{Total} = \sum_{i=1}^{a} \sum_{j=1}^{n} (x_{ij} - \overline{x..})^2$$

$$SS_{Observations} = \frac{1}{n} \sum_{i=1}^{a} x_{i.}^2 - \frac{x..^2}{N}$$

$$SS_{Error} = SS_{Total} - SS_{Observations}$$

where, x.. = Grand total of all observations;
and $\overline{x..}$ = Grand average of all observations

Degree of Freedom (DF)

$$DF_{Total} = a(n) - 1$$

$$DF_{Observations} = a - 1$$

$$DF_{Error} = a(n - 1)$$

Mean Square (MS)

$$MS_{Observations} = \frac{SS_{Observation}}{a-1}$$

$$MS_{Error} = \frac{SS_{Error}}{a(n-1)}$$

$$\text{F-Value} = \frac{MS_{\text{Observations}}}{MS_{\text{Error}}}$$

Comparison of Observation Means

Tukey's Test:

$$q = \frac{\bar{x}_{max} - \bar{x}_{min}}{\sqrt{\frac{MS_{Error}}{n}}}$$

Confidence Interval (C.I):

$$\bar{x}_i - \bar{x}_j - q(a,f)\sqrt{\frac{MS_{Error}}{n}} \leq \mu_i - \mu_j \leq \bar{x}_i - \bar{x}_j + q(a,f)\sqrt{\frac{MS_{Error}}{n}}$$

Fisher–Least Significant Difference (LSD) method

$$t_o = \frac{\bar{x}_{i.} - \bar{x}_{j.}}{\sqrt{MS_{Error}(\frac{1}{ni} + \frac{1}{nj})}}$$

Confidence Interval (C.I):

$$\bar{x}_i - \bar{x}_j - t_{\frac{\alpha}{2}, N-a}\sqrt{MS_{Error}(\frac{1}{ni} + \frac{1}{nj})} \leq \mu_i - \mu_j \leq \bar{x}_i - \bar{x}_j + t_{\frac{\alpha}{2}, N-a}\sqrt{MS_{Error}(\frac{1}{ni} + \frac{1}{nj})}$$

Non-Parametric Test:

Friedman Rank Test:

$$Q = [\frac{12}{n(k)(k+1)} \left(\sum R_j^2\right) - 3n(k+1)]$$

Critical value (k-1, α)

References

1. Dickinson, H. The Next Industrial Revolution? The Role of Public Administration in Supporting Government to Oversee 3D Printing Technologies. *Public Adm. Rev.* **2018**, *78*, 922–925, https://doi.org/10.1111/puar.12988.
2. Gokhare, V.G.; Raut, D.N.; Shinde, D.K. A Review Paper on 3D-Printing Aspects and Various Processes Used in the 3D-Printing. Available online: www.ijert.org (accessed on).
3. Schubert, C.; Van Langeveld, M.C.; A Donoso, L. Innovations in 3D printing: a 3D overview from optics to organs. *Br. J. Ophthalmol.* **2013**, *98*, 159–161.
4. Tay, Y.W.D.; Panda, B.; Paul, S.C.; Mohamed, N.A.N.; Tan, M.J.; Leong, K.F. 3D printing trends in building and construction industry: a review. *Virtual Phys. Prototyp.* **2017**, *12*, 261–276, https://doi.org/10.1080/17452759.2017.1326724.
5. Lafeber, I.; Ruijgrok, E.J.; Guchelaar, H.-J.; Schimmel, K.J.M. 3D Printing of Pediatric Medication: The End of Bad Tasting Oral Liquids?—A Scoping Review. *Pharmaceutics* **2022**, *14*, 416, https://doi.org/10.3390/pharmaceutics14020416.
6. Yan, Q.; Dong, H.; Su, J.; Han, J.; Song, B.; Wei, Q.; Shi, Y. A Review of 3D Printing Technology for Medical Applications. *Engineering* **2018**, *4*, 729–742, https://doi.org/10.1016/j.eng.2018.07.021.
7. Brunner, T.A.; Delley, M.; Denkel, C. Consumers' attitudes and change of attitude toward 3D-printed food. *Food Qual. Preference* **2018**, *68*, 389–396, https://doi.org/10.1016/j.foodqual.2017.12.010.
8. Dawood, A.; Marti, B.M.; Sauret-Jackson, V.; Darwood, A. 3D printing in dentistry. *Br. Dent. J.* **2015**, *219*, 521–529.
9. Barone, S.; Neri, P.; Paoli, A.; Razionale, A.V.; Tamburrino, F. Development of a DLP 3D printer for orthodontic applications. In *Procedia Manufacturing*; Elsevier: Amsterdam, The Netherlands, 2019; pp. 1017–1025, https://doi.org/10.1016/j.promfg.2020.01.187.
10. Gross, B.C.; Erkal, J.L.; Lockwood, S.Y.; Chen, C.; Spence, D.M. Evaluation of 3D Printing and Its Potential Impact on Biotechnology and the Chemical Sciences. *Anal. Chem.* **2014**, *86*, 3240–https://doi.org/10.1021/ac403397r.
11. Štaffová, M.; Ondreáš, F.; Svatík, J.; Zbončák, M.; Jančář, J.; Lepcio, P. 3D printing and post-curing optimization of photopolymerized structures: Basic concepts and effective tools for improved thermomechanical properties. *Polym. Test.* **2022**, *108*, 107499, https://doi.org/10.1016/j.polymertesting.2022.107499.
12. Nguyen, H.T.; Crittenden, K.; Weiss, L.; Bardaweel, H. Experimental Modal Analysis and Characterization of Additively Manufactured Polymers. *Polymers* **2022**, *14*, 2071, https://doi.org/10.3390/polym14102071.
13. Gardan, J.; Makke, A.; Recho, N. A Method to Improve the Fracture Toughness Using 3D Printing by Extrusion Deposition. In *Procedia Structural Integrity*; Elsevier: Amsterdam, The Netherlands, 2016; pp. 144–151, https://doi.org/10.1016/j.prostr.2016.06.019.
14. Chen, Z.; Li, Z.; Li, J.; Liu, C.; Lao, C.; Fu, Y.; Liu, C.; Li, Y.; Wang, P.; He, Y. 3D printing of ceramics: A review. *J. Eur. Ceram. Soc.* **2018**, *39*, 661–687, https://doi.org/10.1016/j.jeurceramsoc.2018.11.013.
15. Shahrubudin, N.; Lee, T.; Ramlan, R. An Overview on 3D Printing Technology: Technological, Materials, and Applications. *Procedia Manuf.* **2019**, *35*, 1286–1296, https://doi.org/10.1016/j.promfg.2019.06.089.
16. Prabhu, S.R.; Ilangkumaran, M.; Mohanraj, T. 3D Printing of automobile spoilers using MCDM techniques. *Mater. Test.* **2020**, *62*, 1121–1125, https://doi.org/10.3139/120.111592.
17. Janeková, J.; Pelle, S.; Onofrejová, D.; Pekarčíková, M. THE 3D PRINTING IMPLEMENTATION IN MANUFACTURING OF AUTOMOBILE COMPONENTS. **2019**, *5*, 17–21, https://doi.org/10.22306/atec.v5i1.49.
18. Elakkad, A.S. 3D Technology in the Automotive Industry. Available online: www.ijert.org (accessed on).
19. Zare, Y.; Rhee, K.Y.; Park, S.-J. A developed equation for electrical conductivity of polymer carbon nanotubes (CNT) nanocomposites based on Halpin-Tsai model. *Results Phys.* **2019**, *14*, 102406, https://doi.org/10.1016/j.rinp.2019.102406.
20. Szabó, L.; Fodor, D. The Key Role of 3D Printing Technologies in the Further Development of Electrical Machines. *Machines* **2022**, *10*, 330, https://doi.org/10.3390/machines10050330.
21. Park, Y.; Yun, I.; Chung, W.G.; Park, W.; Lee, D.H.; Park, J. High-Resolution 3D Printing for Electronics. *Adv. Sci.* **2022**, *9*, 2104623, https://doi.org/10.1002/advs.202104623.

22. Espera, A.H.; Dizon, J.R.C.; Chen, Q.; Advincula, R.C. 3D-printing and advanced manufacturing for electronics. *Prog. Addit. Manuf.* **2019**, *4*, 245–267, https://doi.org/10.1007/s40964-019-00077-7.
23. Leigh, S.J.; Bradley, R.J.; Purssell, C.P.; Billson, D.R.; Hutchins, D.A. A Simple, Low-Cost Conductive Composite Material for 3D Printing of Electronic Sensors. *PLoS ONE* **2012**, *7*, e49365, https://doi.org/10.1371/journal.pone.0049365.
24. Sun, L.; Zhao, L. Envisioning the era of 3D printing: a conceptual model for the fashion industry. *Fash. Text.* **2017**, *4*, 25, https://doi.org/10.1186/s40691-017-0110-4.
25. Wang, B.Z.; Chen, Y. The Effect of 3D Printing Technology on the Future Fashion Design and Manufacturing. *Appl. Mech. Mater.* **2014**, *496*, 2687–2691, https://doi.org/10.4028/www.scientific.net/amm.496-500.2687.
26. Cantrell, J.; et al. Experimental Characterization of the Mechanical Properties of 3D-Printed ABS and Polycarbonate Parts Nomenclature 3D = Three-dimensional AM = Additive manufacturing ABS = Acrylonitrile butadiene styrene ASTM = American Society for Testing and Materials CAD = Computer aided design CI = Confidence interval COV = Coefficient of variation DIC = Digital image correlation FDM = Fused deposition modeling PC = Polycarbonate RP = Rapid prototyping SMP = Shape memory polymer STL = Stereo lithography.
27. Wittbrodt, B.; Pearce, J.M. The effects of PLA color on material properties of 3-D printed components. *Addit. Manuf.* **2015**, *8*, 110–116, https://doi.org/10.1016/j.addma.2015.09.006.
28. Galeta, T.; Raos, P.; Stojšić, J.; Pakši, I. Influence of Structure on Mechanical Properties of 3D Printed Objects. *Procedia Eng.* **2016**, *149*, 100–104, https://doi.org/10.1016/j.proeng.2016.06.644.
29. Lederle, F.; Meyer, F.; Brunotte, G.-P.; Kaldun, C.; Hübner, E.G. Improved mechanical properties of 3D-printed parts by fused deposition modeling processed under the exclusion of oxygen. *Prog. Addit. Manuf.* **2016**, *1*, 3–7, https://doi.org/10.1007/s40964-016-0010-y.
30. Chadha, A.; Haq, M.I.U.; Raina, A.; Singh, R.R.; Penumarti, N.B.; Bishnoi, M.S. Effect of fused deposition modelling process parameters on mechanical properties of 3D printed parts. *World J. Eng.* **2019**, *16*, 550–559, https://doi.org/10.1108/wje-09-2018-0329.
31. Al Khawaja, H.; Mansour, A.; Alabdouli, H.; Ahmed, W.; Alqaydi, H.; Al Jassmi, H. 2020 Advances in Science and Engi-neering Technology International Conferences (ASET).
32. Shemelya, C.; De La Rosa, A.; Torrado, A.R.; Yu, K.; Domanowski, J.; Bonacuse, P.J.; Martin, R.E.; Juhasz, M.; Hurwitz, F.; Wicker, R.B.; et al. Anisotropy of thermal conductivity in 3D printed polymer matrix composites for space based cube satellites. *Addit. Manuf.* **2017**, *16*, 186–196, https://doi.org/10.1016/j.addma.2017.05.012.
33. Laureto, J.; Tomasi, J.; King, J.A.; Pearce, J.M. Thermal properties of 3-D printed polylactic acid-metal composites. *Prog. Addit. Manuf.* **2017**, *2*, 57–71, https://doi.org/10.1007/s40964-017-0019-x.
34. Blanco, I.; Cicala, G.; Recca, G.; Tosto, C. Specific Heat Capacity and Thermal Conductivity Measurements of PLA-Based 3D-Printed Parts with Milled Carbon Fiber Reinforcement. *Entropy* **2022**, *24*, 654, https://doi.org/10.3390/e24050654.
35. Rahim, T.N.A.T.; Abdullah, A.M.; Akil, H.M.; Mohamad, D.; Rajion, Z.A. The improvement of mechanical and thermal properties of polyamide 12 3D printed parts by fused deposition modelling. *Express Polym. Lett.* **2017**, *11*, 963–982, https://doi.org/10.3144/expresspolymlett.2017.92.
36. Pascual-González, C.; Martín, P.S.; Lizarralde, I.; Fernández, A.; León, A.; Lopes, C.; Fernández-Blázquez, J. Post-processing effects on microstructure, interlaminar and thermal properties of 3D printed continuous carbon fibre composites. *Compos. Part B: Eng.* **2021**, *210*, 108652, https://doi.org/10.1016/j.compositesb.2021.108652.
37. Rynio, P.; Wojtuń, M.; Wójcik, .; Kawa, M.; Falkowski, A.; Gutowski, P.; Kazimierczak, A. The accuracy and reliability of 3D printed aortic templates: a comprehensive three-dimensional analysis. *Quant. Imaging Med. Surg.* **2022**, *12*, 1385–1396, https://doi.org/10.21037/qims-21-529.
38. Siraj, I.; Bharti, P.S. Reliability analysis of a 3D Printing process. *Procedia Comput. Sci.* **2020**, *173*, 191–200, https://doi.org/10.1016/j.procs.2020.06.023.
39. Keleş, .; Blevins, C.W.; Bowman, K.J. Effect of build orientation on the mechanical reliability of 3D printed ABS. *Rapid Prototyp. J.* **2017**, *23*, 320–328, https://doi.org/10.1108/rpj-09-2015-0122.
40. Goh, G.D.; Sing, S.L.; Yeong, W.Y. A review on machine learning in 3D printing: applications, potential, and challenges. *Artif Intell. Rev.* **2021**, *54*, 63–94.
41. Wu, H.-C.; Chen, T.-C.T. Quality control issues in 3D-printing manufacturing: a review. *Rapid Prototyp. J.* **2018**, *24*, 607–614, https://doi.org/10.1108/rpj-02-2017-0031.
42. Song, X.; Liu, H.; Fang, Y.; Zhao, C.; Qu, Z.; Wang, Q.; Tu, L.-C. An Integrated Gold-Film Temperature Sensor for In Situ Temperature Measurement of a High-Precision MEMS Accelerometer. *Sensors* **2020**, *20*, 3652, https://doi.org/10.3390/s20133652.
43. Li, Y.; Zhao, W.; Li, Q.; Wang, T.; Wang, G. In-Situ Monitoring and Diagnosing for Fused Filament Fabrication Process Based on Vibration Sensors. *Sensors* **2019**, *19*, 2589, https://doi.org/10.3390/s19112589.
44. Noda, T.; Kawabata, Y.; Arai, N.; Mitamura, H.; Watanabe, S. Animal-Mounted Gyroscope/Accelerometer/Magnetometer: In Situ Measurement of the Movement Performance of Fast-Start Behaviour in Fish. 2013. Available online: http://www.elsevier.com/open-access/userlicense/1.0/http://www.elsevier.com/open-access/userlicense/1.0 (accessed on).
45. Schleier, M.; Adelmann, B.; Esen, C.; Hellmann, R. Image Processing Algorithm for In Situ Monitoring Fiber Laser Remote Cutting by a High-Speed Camera. *Sensors* **2022**, *22*, 2863, https://doi.org/10.3390/s22082863.
46. Grasso, M.; Colosimo, B.M. Process defects and*in situ*monitoring methods in metal powder bed fusion: a review. *Meas. Sci. Technol.* **2017**, *28*, 044005, https://doi.org/10.1088/1361-6501/aa5c4f.

47. Wu, H.; Wang, Y.; Yu, Z. In situ monitoring of FDM machine condition via acoustic emission. *Int. J. Adv. Manuf. Technol.* **2016**, *84*, 1483–1495, https://doi.org/10.1007/s00170-015-7809-4.
48. De Rosa, I.M.; Sarasini, F. Use of PVDF as acoustic emission sensor for in situ monitoring of mechanical behaviour of glass/epoxy laminates. *Polym. Test.* **2010**, *29*, 749–758, https://doi.org/10.1016/j.polymertesting.2010.04.006.
49. Nam, J.; Jo, N.; Kim, J.S.; Lee, S.W. Development of a health monitoring and diagnosis framework for fused deposition modeling process based on a machine learning algorithm. *Proc. Inst. Mech. Eng. Part B: J. Eng. Manuf.* **2019**, *234*, 324–332, https://doi.org/10.1177/0954405419855224.
50. Chang, T.; Mukherjee, S.; Watkins, N.N.; Stobbe, D.M.; Mays, O.; Baluyot, E.V.; Pascall, A.J.; Tringe, J.W. In-situ monitoring for liquid metal jetting using a millimeter-wave impedance diagnostic. *Sci. Rep.* **2020**, *10*, 1–9, https://doi.org/10.1038/s41598-020-79266-2.
51. Dressler, M.; Röllig, M.; Schmidt, M.; Maturilli, A.; Helbert, J. Temperature distribution in powder beds during 3D printing. *Rapid Prototyp. J.* **2010**, *16*, 328–336, https://doi.org/10.1108/13552541011065722.
52. Woszczyński, M.; Rogala-Rojek, J.; Bartoszek, S.; Gaiceanu, M.; Filipowicz, K.; Kotwica, K. In Situ Tests of the Monitoring and Diagnostic System for Individual Photovoltaic Panels. *Energies* **2021**, *14*, 1770, https://doi.org/10.3390/en14061770.
53. Fu, Y.; Downey, A.; Yuan, L.; Pratt, A.; Balogun, Y. In situ monitoring for fused filament fabrication process: A review. *Addit. Manuf.* **2021**, *38*, 101749, https://doi.org/10.1016/j.addma.2020.101749.
54. Dawoud, M.; Taha, I.; Ebeid, S.J. Mechanical behaviour of ABS: An experimental study using FDM and injection moulding techniques. *J. Manuf. Process.* **2016**, *21*, 39–45, https://doi.org/10.1016/j.jmapro.2015.11.002.
55. Yousefi, A.A. Effects of 3D Printer Nozzle Head Temperature on the Physical and Mechanical Properties of PLA Based Product. 2016. Available online: https://www.researchgate.net/publication/309721923 (accessed on).
56. Rankouhi, B.; Javadpour, S.; Delfanian, F.; Letcher, T. Failure Analysis and Mechanical Characterization of 3D Printed ABS With Respect to Layer Thickness and Orientation. *J. Fail. Anal. Prev.* **2016**, *16*, 467–481, https://doi.org/10.1007/s11668-016-0113-2.
57. Christiyan, K.G.J.; Chandrasekhar, U.; Venkateswarlu, K. A study on the influence of process parameters on the Mechanical Properties of 3D printed ABS composite. In Proceedings of the IOP Conference Series: Materials Science and Engineering, Bali, Indonesia, 19–20 March 2016; doi:10.1088/1757-899X/114/1/012109.